Electrical Engineering (2006) 88: 183–190
DOI 10.1007/s00202-004-0275-x

ORIGINAL PAPER

Z. Radakovic · E. Cardillo · M. Schaefer · K. Feser

Design of the winding–bushing interconnections in large power transformers

Received: 24 May 2004 / Accepted: 9 October 2004 / Published online: 20 July 2005

Abstract The paper presents the improvement in design of the conductor connecting the windings and bushings in oil power transformers. This is a sensitive part of large transformers and there is a need to optimise its manufacturing time and costs. The thermal problem of the heating of this conductor with increased insulation thickness on a part of it is treated using a non-linear two-dimensional thermal model. The experiments performed made determining of some problematic parameters (heat resistance of oil-paper insulation and the paper to oil convection heat transfer coefficient) of the thermal model feasible. The results obtained are of practical interest in the design practice of interconnections, but also affect the important parameters of heat transfer by devices with oil immersed paper insulation.

Keywords Winding interconnection · Additional insulation · Temperature calculation

List of symbols

Δx (m)	Length of a finite conductor element (0.1 m)
$a \times b$ (m^2)	Copper cross-section dimensions (17×22 mm)
δ_p (m)	Paper insulation thickness
Subscript *	With normal insulation
Subscript **	With additional insulation (equivalent value Eq. 14)
δ_a (m)	Thickness of the additional manually wrapped insulation
ϑ_O (°C)	Oil temperature
ϑ_a (°C)	Ambient (air) temperature
q_{Cui} (W)	Power losses in the ith finite element
ϑ_{Cui} (°C)	Conductor temperature of the ith finite element
ϑ_{Pi} (°C)	Insulation temperature of the ith finite element
$R_{\lambda Pi}$ (K W^{-1})	Thermal resistance of conduction through paper insulation
$R_{\alpha i}$ (K W^{-1})	Thermal resistance of convection from the paper's insulation outer surface to the surrounding oil
$R_{\lambda Cu}$ (K W^{-1})	Thermal resistance of conductive heat transfer through the copper
k_s	Skin and proximity effect coefficient
S_{Cu} (m^2)	Total conductor cross section (263.25 mm^2)
ρ_{Cu20} (Ω m)	Specific electrical copper resistance at 20°C (1.7×10^{-8} Ω m)
α_{Cu20} (°C^{-1})	Thermal coefficient of resistance (3.9×10^{-3}°C^{-1})
I (A)	Current
λ_{Cu} (W m^{-1} K^{-1})	Thermal conductivity of copper (401 W m^{-1} K^{-1})
α_i (W m^{-2} K^{-1})	Convection heat transfer coefficient
S_{po} (m^2)	Convection heat transfer surface
Ra	Rayleigh number
Nu	Nusselt number
D (m)	Cylinder diameter, i.e. equivalent diameter of the conductor
ϑ_s (°C)	Cylinder surface temperature
ϑ_f (°C)	Fluid temperature
g (m s^{-2})	Gravitational acceleration (9.81 m s^{-2})
β (K^{-1})	Oil volumetric thermal expansion coefficient
ν (m s^{-2})	Oil kinematic viscosity
a (m^2 s^{-1})	Oil thermal diffusivity

Z. Radakovic (✉)
Siemens AG PTD T TI, Katzwanger Strasse 150,
90461 Nuernberg, Germany
E-mail: zoran.radakovic@siemens.com

E. Cardillo · K. Feser
Institute of Power Transmission and High Voltage Technology (IEH), Pfaffenwaldring 47, 70569 Stuttgart-Vaihingen, Germany
E-mail: enzo.cardillo@ieh.uni-stuttgart.de
E-mail: kurt.feser@ieh.uni-stuttgart.de

M. Schaefer
Siemens AG PTD T PN O, Katzwanger Strasse 150,
90461 Nuernberg, Germany
E-mail: michael.m.schaefer@siemens.com

λ (W m^{-1} K^{-1})	Oil thermal conductivity
Pr	Oil Prandtl number
ϑ_{par} (°C)	Average surface and oil temperature
λ_P (W m^{-1} K^{-1})	Thermal conductivity of the oil-paper insulation (0.0015 W m^{-1} K^{-1})
S_P (m^2)	Cross section of heat conduction through the paper area
$\vartheta_{s\ i}$ (°C)	Temperature measured by the sensor at position i (i=0,1,2,...,28)
ϑ (°C)	Temperature
J (A mm^{-2})	Current density
ϑ_{ac} (°C)	Calculated mean winding temperature
ϑ_{am} (°C)	Measured mean winding temperature
$\Delta\ \vartheta_a$ (K)	Deviation of calculated from measured mean winding temperature
ϑ_{Oa} (°C)	Average oil temperature
$\Delta\ \vartheta_{si}$ (K)	Difference between calculated and measured temperature values at measuring positions in the insulation

1 Introduction

Conductors used for transformer winding interconnections usually need higher insulation levels than the insulation inside windings. In practice, the insulation on short segments of the winding interconnections is several times thicker than the insulation inside windings. This leads to increased conductor temperature rises. To avoid unacceptable high temperatures inside winding interconnections, conductors with an increased cross section are used to decrease power losses inside parts with additional insulation. The normally used design rules assume an infinite length of the additionally insulated conductor. In a number of cases the conductor length equipped with an additional insulation is less than half a meter. In such short conductor segments the heat flow along the conductor is not negligible compared with the heat flow through the conductor insulation. A two-dimensional thermal model is needed to calculate the temperature precisely. With such a model, it is possible to determine the minimum cross section leading to acceptable values of local hottest insulation temperature. Some savings in a manufacturing process of costly connections, always representing a risk of failure, can be achieved.

2 Thermal model

The steady-state thermal model is established using the finite-element (FE) method. The system is two dimensional and non-linear. One dimension of heat transfer is in the axial direction along the conductor (conduction through copper) and the other is perpendicular to the conductor (conduction through the paper insulation and convection from the winding surface to surrounding oil). The non-linearity originates from the variation of the convection heat transfer coefficient with the temperature.

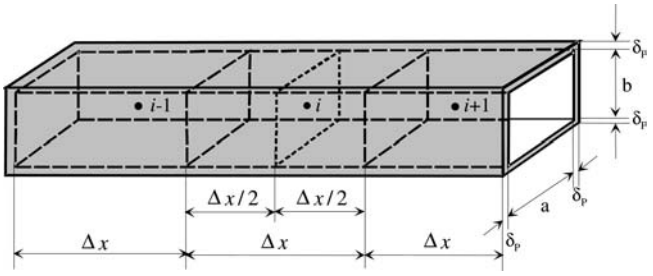

Fig. 1 Finite elements of the conductor

A conductor element (i) of length Δx adjoined from the left ($i-1$) and from the right ($i+1$) sides by elements of the same length (see Fig. 1) is considered.

For the ith element, the thermal network shown in Fig. 2 can be drawn up.

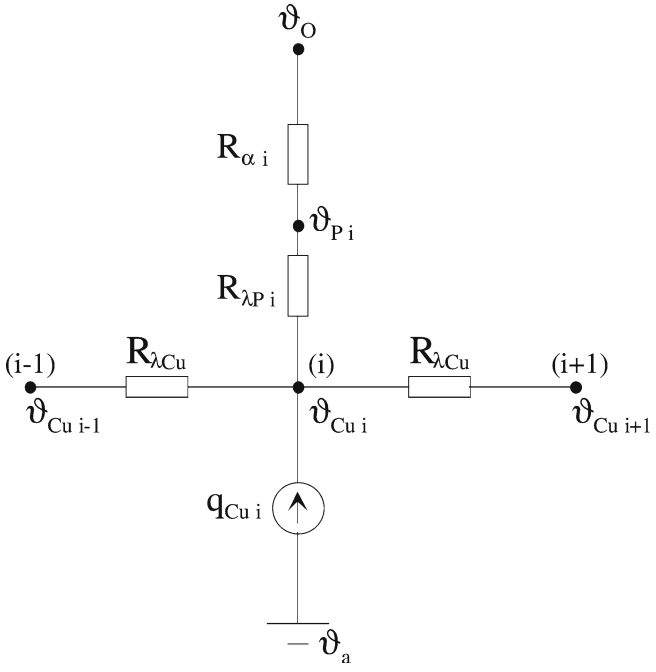

Fig. 2 Thermal network for one conductor finite element

Symbol	Meaning
ϑ_{Cui}	Copper temperature of the ith element (part) (°C)
$\vartheta_{Cu}i-1$	Copper temperature of the ($i-1$)th element (°C)
ϑ_{Cui+1}	Copper temperature of the ($i+1$)th element (°C)
ϑ_{pi}	Paper insulation outer surface temperature of the ith element (°C)
ϑ_O	Oil temperature (°C)
ϑ_a	Ambient temperature (°C)
q_{Cui}	Power losses in the ith element (W)
$R_{\lambda Cu}$	Thermal resistance of conductive heat transfer through the copper (K W^{-1})
$R_{\lambda Pi}$	Thermal resistance of conductive heat transfer through the paper insulation (K W^{-1})
$R_{\alpha i}$	Thermal resistance of convection heat transfer from the paper surface to the surrounding oil (K W^{-1})

$$q_{\mathrm{Cu}i} = k_{\mathrm{s}}\rho_{\mathrm{Cu20}}(1 + \alpha_{\mathrm{Cu20}}(\vartheta_{\mathrm{Cu}i} - 20^{\circ}\mathrm{C}))\frac{\Delta x}{S_{\mathrm{Cu}}}I^2; \quad (1)$$

$$R_{\lambda\mathrm{Cu}} = \frac{1}{\lambda_{\mathrm{Cu}}}\frac{\Delta x}{S_{\mathrm{Cu}}}; \quad (2)$$

$$R_{\alpha i} = \frac{1}{\alpha_i S_{\mathrm{po}}}, \quad (3)$$

$$S_{\mathrm{po}} = 2\,(a + 2\,\delta_{\mathrm{p}} + b + 2\,\delta_{\mathrm{p}})\,\Delta x. \quad (4)$$

Symbol	Meaning
k_{s}	Skin and proximity effect coefficient
ρ_{Cu20}	Specific electrical copper resistance at 20°C (Ω m)
α_{Cu20}	Thermal coefficient of resistance ($^{\circ}\mathrm{C}^{-1}$)
S_{Cu}	Total conductor cross section (m^2)
I	Current (A)
λ_{Cu}	Thermal conductivity of copper (W m^{-1} K^{-1})
α_i	Convection heat transfer coefficient (W m^{-2} K^{-1})
S_{po}	Convection heat transfer surface (m^2)
$a \times b$	Conductor copper dimensions (m^2)
δ_{p}	Paper insulation thickness (m)

The equations for the convection heat transfer coefficient α_i for a horizontal bar immersed in a fluid can be found in heat transfer literature [1]. The calculation procedure through Rayleigh (Ra) and Nusselt (Nu) numbers for a horizontal cylinder with diameter D and cylinder surface and fluid temperatures ϑ_{s} and ϑ_{f} can be approximately applied to the bar of non-circulate cross section if the equivalent diameter D is set to $(S_{\mathrm{po}}/\Delta x)/\pi$. The Rayleigh number is defined by

$$\mathrm{Ra} = \frac{g\beta(\vartheta_{\mathrm{s}} - \vartheta_{\mathrm{f}})D^3}{va}. \quad (5)$$

By [2], valid for $\mathrm{Ra} \le 10^{12}$,

$$\mathrm{Nu} = \left(0.60 + \frac{0.387\mathrm{Ra}^{1/6}}{\left[1 + \left(\frac{0.559}{\mathrm{Pr}}\right)^{9/16}\right]^{8/27}}\right)^2 \quad (6)$$

and by [3]

$$\mathrm{Nu} = C\ \mathrm{Ra}^n, \quad (7)$$

where for $10^4 \le \mathrm{Ra} \le 10^7$, the values for the coefficients are $C = 0.480$ and $n = 0.250$. The heat transfer coefficient is equal to

$$\alpha = \frac{\lambda \mathrm{Nu}}{D}. \quad (8)$$

All fluid parameters are taken at mean surface and oil temperature:

$$\vartheta_{\mathrm{par}} = \frac{\vartheta_{\mathrm{s}} + \vartheta_{\mathrm{f}}}{2}. \quad (9)$$

Symbol	Meaning
ν	Kinematic viscosity (m^2 s^{-1})
a	Thermal diffusivity (m^2 s^{-1})
g	Gravitational acceleration (9.81 m s^{-2})
β	Volumetric thermal expansion coefficient (K^{-1})
Pr	Prandtl number, equal to ν/a
λ	Thermal conductivity (W m^{-1} K^{-1})

Based on Fig. 2, the following equation for the ith element can be written:

$$\frac{\vartheta_{\mathrm{Cu}i-1} - \vartheta_{\mathrm{Cu}i}}{R_{\lambda\mathrm{Cu}}} + \frac{\vartheta_{\mathrm{Cu}i+1} - \vartheta_{\mathrm{Cu}i}}{R_{\lambda\mathrm{Cu}}} + q_{\mathrm{Cu}i} = \frac{\vartheta_{\mathrm{Cu}i} - \vartheta_{\mathrm{o}}}{R_{\lambda\mathrm{P}i} + R_{\alpha i}(\vartheta_{\mathrm{p}i}, \vartheta_{\mathrm{o}})}. \quad (10)$$

The values of $R_{\alpha i}$ are calculated using Eqs. 3, 4, 5, 6 or Eqs. 7 and 8; ϑ_{s} in these equations corresponds to the temperature $\vartheta_{\mathrm{p}\ i}$. To complete the system of equations, the relation between the temperatures $\vartheta_{\mathrm{Cu}\ i}$ and $\vartheta_{\mathrm{p}\ i}$ is necessary. From Fig. 2, it can be deduced that

$$\vartheta_{\mathrm{P}i} = \vartheta_{\mathrm{Cu}i} - R_{\lambda\mathrm{P}i}\frac{\vartheta_{\mathrm{Cu}i} - \vartheta_{\mathrm{o}}}{R_{\lambda\mathrm{P}i} + R_{\alpha i}(\vartheta_{\mathrm{p}i}, \vartheta_{\mathrm{o}})}. \quad (11)$$

The system of equations, even for this single node, is complex. Therefore, the use of numerical methods and computer calculations is necessary for solving.

The same equations can be generated for other elements of length Δx ($i = 1, 2, \ldots, n$). It is assumed that the temperature of the boundary surfaces—on the first and the last (nth) element—are known.

Solving this non-linear system of $2n$ equations, wherein the convection thermal resistances are temperature dependent, the values of $\vartheta_{\mathrm{Cu}\ i}$ and $\vartheta_{\mathrm{P}\ i}$ ($i = 1, 2, \ldots, n$) can be calculated.

3 Discussion on thermal model application

The structure of the model exposed is well known, but there are some practical problems in its application:

- Thermal resistance $R_{\lambda\mathrm{P}\ i}$ calculation
- Thermal resistance $R_{\alpha i}$, i.e. convection heat transfer coefficient α_i, calculation
- Boundary condition definition

It is known [4] that the thermal resistance $R_{\lambda\mathrm{P}\ i}$ cannot be calculated using

$$R_{\lambda Pi} = \frac{1}{\lambda_p}\frac{\delta_p}{S_P}, \tag{12}$$

where λ_p denotes the thermal conductivity of the oil-paper insulation and S_p the mean paper cross section, which is equal to

$$S_p = 2\,(a + \delta_p + b + \delta_p)\Delta x. \tag{13}$$

The thickness of the additional paper layers wrapped up on the typical conductor, used in the experiments, was only 60% of the thickness determined from outer dimension. The rest of space (40%) is filled with air, which has approximately six times lower thermal conductivity than the paper. Of course, during the vacuuming process, a certain quantity of air is removed and the space between the paper layers is filled up with oil. It means that the thermal resistance of the oil-paper insulation system consists of various elements, whose contribution to the total thermal resistance cannot be determined in a theoretical way [5].

The problem of α_i calculation will now be illustrated in the succeeding example. A horizontal cylinder in oil is considered, with the following data:

Diameter	$D = 24.83$ mm
Surface temperature	$\vartheta_s = 41$°C
Oil temperature	$\vartheta_f = 35$°C
Mean temperature	$\vartheta_{par} = 38$°C
Oil parameters	$\nu = 1.064\times10^{-5}$ m^2 s^{-1}
	$a = 7.48\times10^{-8}$ m^2 s^{-1}
	$\beta = 0.7464\times10^{-3}$ K^{-1}
	$\lambda = 0.13$ W m^{-1} K^{-1}

Using Eqs. 5, 6 and 8 leads to $\alpha_1 = 97.4$ W m^{-2} K^{-1}, and Eqs. 5, 7 and 8 to $\alpha_2 = 76.2$ W m^{-2} K^{-1}. Using Eq. 6 delivers 27.8% higher results than using Eq. 7.

The problem with the boundary conditions is unknown temperature at the endings of the conductor. In the practical case considered, these temperatures were measured, and consequently known. In real situations, as a rough conservative approximation, the hot-spot temperature of the winding (according to [6], for example) can be adopted. A higher accuracy would be reached by extending the thermal model to the location of the hot-spot temperature, which is somewhat below the top of the winding. In this extension of the model, a simplified presentation of the heat transfer in the winding can be used (one additional node). Also, instead of the value of the hot-spot temperature of the winding, a better estimation of the bushing temperature can be made for the second boundary condition.

4 Experiment

The continuous transposed conductor is of a cross-section of 263.25 mm^2; the skin and proximity effect coefficient is estimated based on the data from cable handbook [7] as $k_s = 1.02$. The length of the investigated conductor sample is 1.4 m. It was placed in a tank filled with transformer oil. Eleven temperature sensors (PT 100) with 10 cm distance were installed along the vertical side of the conductor. They were mounted directly on the enamel of the conductor after cutting out appropriate small areas of insulation (5×4 mm). In the case of normal insulation, the sensors were not covered by the paper, in contrary to the case of thick additional insulation. Only the central part of the conductor with a length of 1.1 m was wrapped with paper insulation. Two additional sensors were fixed outside the paper insulated area (sensors number 0 and 12). The corresponding temperature sensors in the oil were mounted at the same vertical height. The distance between copper surface and oil temperature sensors is 20 mm. As shown in Fig. 3, three additional temperature sensors were installed to measure temperatures of bottom oil, top oil and ambient air. The designation ϑ_{si} is used to denote the temperature value at sensor position i ($i = 0, 1, 2, \ldots, 28$).

The outlook of the experimental set-up is shown in Fig. 4.

The temperatures were measured by a prototype transformer monitoring system [8]. The tank was filled with mineral transformer oil. Based on the values of oil parameters at different temperatures, the following analytical expressions were derived:

$$\lambda(\vartheta) = 0.1326 - 0.00007\vartheta$$

$$\mathrm{Pr}(\vartheta) = 4771\vartheta^{-0.888} - 46.461$$

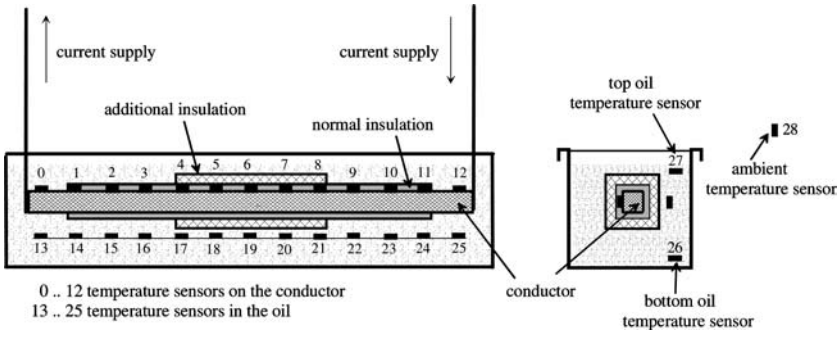

Fig. 3 Sensor positions

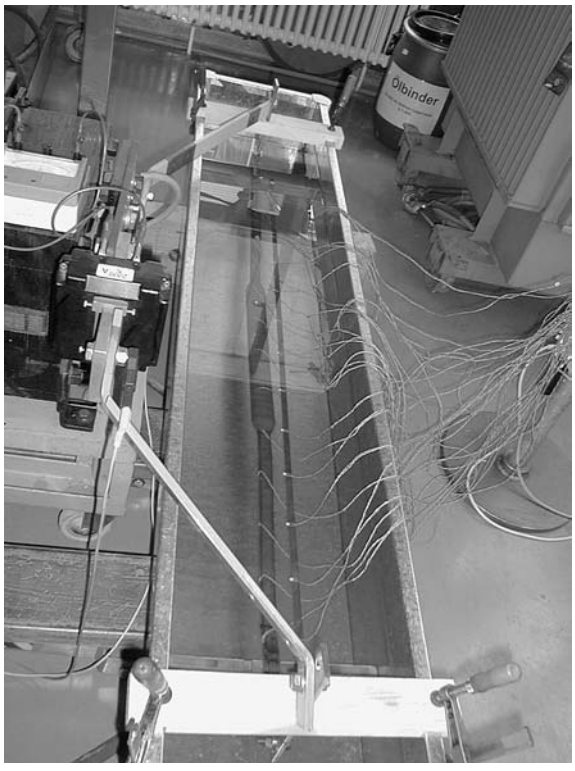

Fig. 4 The outlook of the experimental set-up

$$v(\vartheta) = (334.96\vartheta^{-0.848} - 4.684)10^{-6}$$

$$\beta(\vartheta) = (0.729 + 0.0006212(\vartheta - 10))10^{-3}$$

The quoted expressions deliver values of oil parameters with an error under 1.6% in the temperature (ϑ) range from 25°C to 75°C.

The experiments were carried out in two steps. The first group of experiments was the heating of the conductor with normal insulation for current densities (J) of 1 A mm^{-2} to 6 A mm^{-2}, in steps of 0.5 A mm^{-2}. All copper to oil temperature differences were measured when their steady-state value was reached. After that, additional insulation of a thickness δ_a and a length 40 cm was wrapped in the middle of the conductor. The same sequence of experiments was repeated. Only the experiment with 6 A mm^{-2} was not possible to perform because the insulation temperature exceeded 125°C (adopted limit) before the copper to oil temperature difference reached its steady-state value.

The load current of about 1600 A was provided in laboratory conditions with a single phase transformer. The supply circuit was formed by copper bus bars. The bus bar cross section was bigger than required for 1600 A and the loop was made as small as possible in order to reduce the resistance and the inductance. Also, the contacts were formed carefully in order to minimize the voltage drop and local heating at the end of the conductor. The elements of the experimental set-up are shown in Fig. 5.

5 Application of the model

5.1 Experimental evaluation of the parameters

5.1.1 Convection heat transfer coefficient

The evaluation of the convection heat transfer coefficient was done from the results of measurements on the conductor with normal insulation of thickness δ_p^*. The nodes of the model in which temperatures are calculated correspond exactly to the spots where temperatures were measured. In these calculations, all nodes in the complete thermal circuit represent the same volume (parts left and right from the node, each of length $\Delta x/2$).

Since the paper insulation is wrapped in the factory manufacturing process of the conductor, the values of $R_{\lambda P\,i}$ are calculated using the elementary expression (12).

Two different calculations were made: the first using expression (6) and the second using expression (7). The

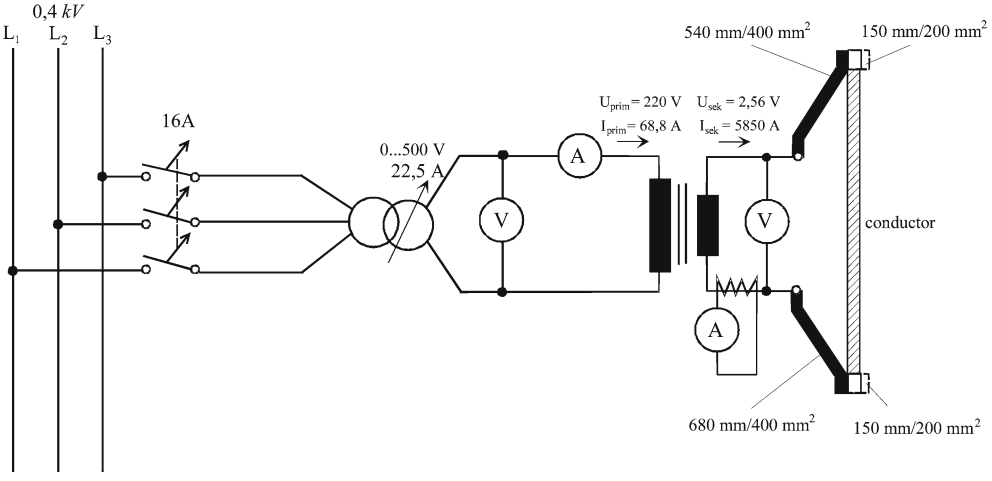

Fig. 5 Electrical scheme

calculated and measured mean copper minus mean oil temperature differences are shown in Fig. 6. The measured copper values are defined as the mean values of the 11 measured temperatures in the paper insulation and the calculated copper temperatures are defined as the mean values of the 11 calculated local conductor temperatures. The measured copper temperatures are all similar, i.e. there is no significant temperature variation along the bar; such a variation could be caused by the direct contact of the copper and the oil at the ends of the conductor.

The calculation of Nusselt number by Eq. 6 (causing maximum calculation error of temperature 5.4 K) leads to more accurate results than by Eq. 7 (causing maximum calculation error of temperature 9.1 K); note that the formula (6) has a lower absolute accuracy at higher current densities. It is possible to correct the expression for Nusselt number to get more accurate calculated temperature values, but there is no particular sense since the influence of the Nusselt number on the copper temperature values is not high. For example, for the current density of 3.5 A mm^{-2} the average steady-state temperatures of copper and oil are 52.2°C and 40.4°C. The calculation of the copper temperature using Eqs. 5, 6 and 8 leads to an average conductor temperature of 53.3°C with the convection heat transfer coefficient of 97.1 W m^{-2} K^{-1}. If α would have the value $\alpha = 115.5$ W m^{-2} K^{-1}, the calculated copper temperature would be with zero error, equal to 52.2°C. It means that an increase of the coefficient α of 18.9% leads to the temperature rise decrease of 1 K, i.e.

$$\frac{53.3°\mathrm{C} - 52.2°\mathrm{C}}{52.2°\mathrm{C} - 40.4°\mathrm{C}} = 9.3\%.$$

The slight influence of the value of convection heat transfer coefficient to the accuracy of calculation of the hot-spot temperature is pointed out in [9].

One simple correction, the change of the coefficient 1/6 in Eq. 6 to 1/5, improves the calculation accuracy as shown in Fig. 6 (curve "corrected Eq. 6"). It means that the real values of the convection heat transfer coefficients are higher than that obtained from Eq. 6, which is the general expression established in heat transfer theory. The underestimation of convection heat transfer coefficients with Eq. 6 is obvious from Fig. 6. As the figure shows, the error is growing up with the power density, i.e. with the paper to oil temperature difference.

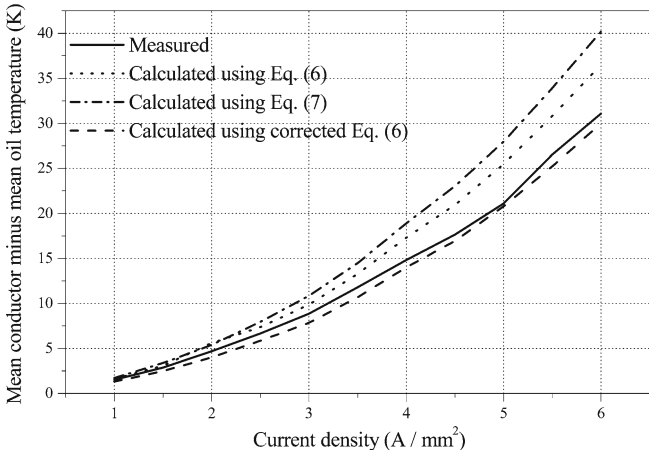

Fig. 6 Calculated and measured mean winding minus mean oil temperature differences

It would be desirable to check the validity of the formula in real transformers since the oil streaming conditions in transformers differ from those in the experiment. The origin of the forces is also in the active part of the transformer—windings and the core. In addition, it is sensitive to the temperature which is applied to the top oil [10].

5.1.2 Thermal resistance of manually wrapped additional insulation

As stated in Sect. 3, the manually wrapped insulation consists of various elements (paper, oil, air), whose contribution to the total thermal resistance cannot be determined in a theoretical way. As the solution, the following principle is applied. The values of the thermal resistance of conductive heat transfer through the paper insulation is calculated by Eq. 12, where the paper insulation thickness δ_p is equal to the sum of normal paper insulation and thickness of additional insulation (δ_a) multiplied by a factor greater than 1. The value of the coefficient is determined so as to achieve good agreement between the calculated and measured values of copper temperatures in experiments done on the conductor with additional paper insulation.

The model for the calculation of the temperatures for the conductor with additional insulation is built with the same nodes as in the series of calculations for the conductor with normal insulation, but the volumes of the conductor corresponding to the nodes were changed. The nodes at the edge of the additional insulation (nodes 4 and 8 in Fig. 3) represent the part $\Delta x/2$ width and additionally insulated. Nodes with normal insulation adjacent to the section with the additional insulation (nodes 3 and 9 in Fig. 3) represent the part $\Delta x + \Delta x/2$ width with normal insulation. In that way, the paralleling of thermal resistances of the heat transfer through the insulation of normal and increased thickness is avoided. These changes reflect to the surface, thermal resistances of conduction through paper and convection, as well as to the values of heat sources. For example, for nodes 4 and 8, the surface is reduced to half, the thermal resistances are doubled and the power loss is reduced to half, all compared with the values for nodes 5, 6 and 7.

The values of $R_{\lambda P\ i}$ for nodes which represent elements with normal insulation thickness are calculated in the same way as in the series of calculations of the temperatures for the conductor with normal insulation.

For nodes 4, 5, 6, 7 and 8, Eq. 12 was used where δ_p is adopted as the thickness of normal paper insulation plus

thickness of additional insulation (δ_a) multiplied by the factor 1.5:

$$\delta_p^{**} = \delta_p^* + 1.5 \times \delta_a \quad (14)$$

The value of 1.5 is adopted as it results in a good agreement between the calculated and measured temperatures (see Fig. 7). Since the value for the factor is obtained from the results of measurements done on the typically manufactured conductor, it could be recommended as a value to be applied in other calculations of interconnections in oil power transformers. The surface values for nodes 4, 5, 6, 7 and 8 are

$$S_p = 2(a + \delta_p^* + \delta_a + b + \delta_p^* + \delta_a)l;$$

for nodes 5, 6 and 7, $l = \Delta x$ and for nodes 4 and 8, $l = \Delta x/2$.

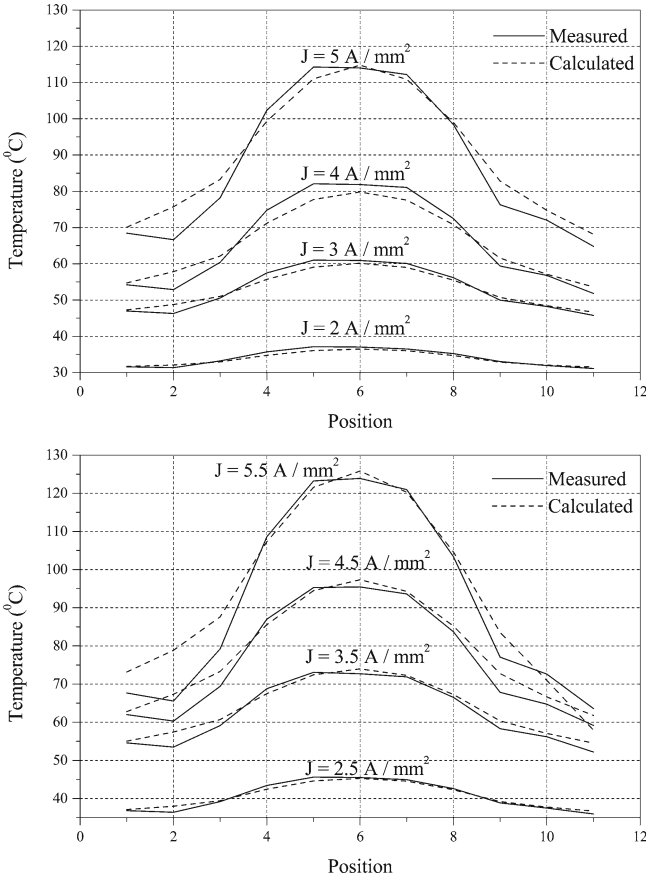

Fig. 7 Calculated and measured conductor temperature distribution: additional insulation

5.2 Comparison of measured and calculated temperatures

The results of the calculation of the temperatures for the conductor with uniform (normal) insulation are shown in Fig. 6.

The input data, i.e. the model boundary conditions, for the calculations of the temperatures for the conductor with additional insulation are presented in Table 1: the average measured oil temperatures (ϑ_{Oa}) and the copper temperatures at positions 0 (ϑ_{s0}) and 12 (ϑ_{s12}).

Figure 7 presents the calculation results for the conductor with additional insulation.

In the most important region of the highest temperatures (part with additional insulation, nodes 4–8), the calculated temperatures match very well with the measured values.

5.3 Discussion of temperature distribution along the conductor

The aim of the research was to develop the design method of the conductor with additional insulation on a part of it. The cross section is selected to remain the hottest spot of the insulation below the allowed limit. Consequently, results and analysis of the hottest spot will be exposed. Figure 8 shows the measured insulation hottest spot minus oil temperature for both cases: the conductor with normal and with additional insulation.

Increased hottest spot temperatures by the conductor with additional insulation are the consequence of: (a) the temperature drop due to heat transfer through the copper in the part with additional insulation; the heat transferred through the additional insulation is much lower and (b) comparing to the case of normal insulation, the effective cooling surface through which the heat is transferred to the oil is reduced (approximately from 1.1 m to 0.7 m—it means down to 64%).

In Fig. 9, the results of two calculation methods are shown. In the simplified, commonly used method, the temperature rise is calculated as the product of the power loss per unit length and the thermal resistance of the heat conduction through the additional insulation per unit length. It is clear that the simplified calculation is too vague and leads to high dimensions of interconnections. On the other side, the model proposed in the paper delivers the hottest spot temperature with a high accuracy and enables a precise design of the cross section.

Table 1 Model boundary conditions

J (A mm^{-2})	1	1.5	2	2.5	3	3.5	4	4.5	5	5.5	6
ϑ_{Oa} (°C)	31.3	34.5	26.2	29.1	36.6	41.4	36.9	41.4	43.5	38.4	–
ϑ_{s0} (°C)	31.4	36.3	31.3	36.3	45.6	52.3	51.2	57.3	63.6	67.6	–
ϑ_{s12} (°C)	32.7	36.3	31.0	35.6	44.7	51.5	49.4	55.6	60.1	38.37	–

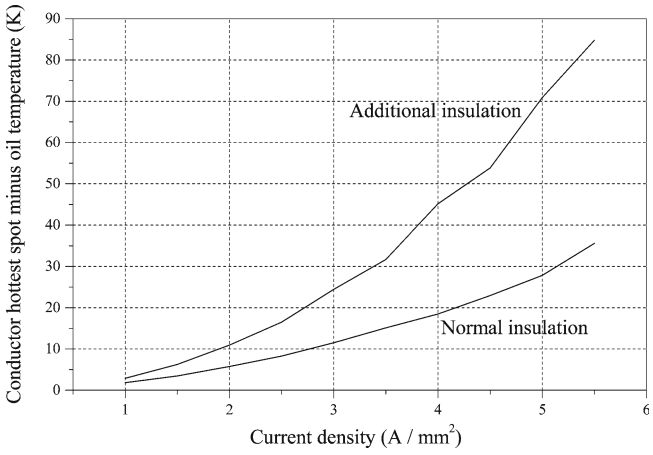

Fig. 8 Temperature difference dependence on current density

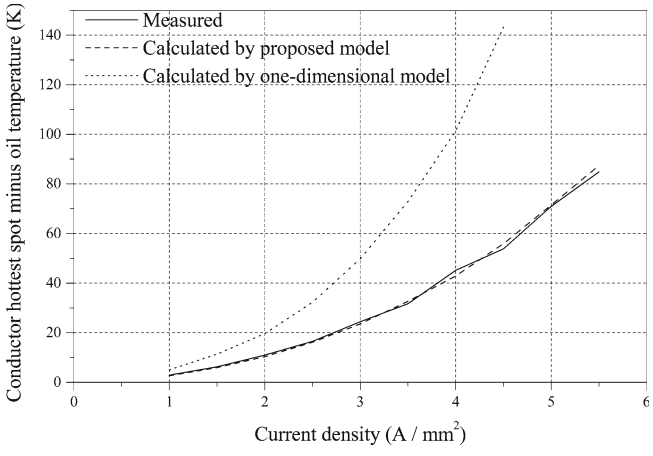

Fig. 9 Measured and calculated hot spot to oil temperature rise: additional insulation

In the following example, the effect of a precise temperature calculation to the design of the interconnection will be exposed. For an adopted temperature difference of the conductor hottest-spot minus oil temperature of 23 K (according to [6]), the conductor can be loaded with $J_1 = 2.13$ A mm^{-2} calculated by the simplified method and with $J_2 = 2.97$ A mm^{-2} calculated with the proposed model. It means that the application of the proposed precise and less conservative model permits the reduction of the cross section of the interconnections to 100 $J_1/J_2 = 72\%$.

6 Conclusions

The application of the non-linear two-dimensional model is proved as a good modern method for the design of interconnections (conductor connecting the windings and bushings) inside large oil power transformers. The calculation method proposed represents an improvement in design practice and leads to techno-economically optimal construction of the interconnections. The method was verified in laboratory experiments on a conductor with a cross section of 263 mm^2, loaded with currents up to 1,450 A.

Based on the experiments, the correction of the formula for convection heat transfer for horizontal bar [2] was given. Another important recommendation of a general interest is the one for thermal resistances of conduction through manually wrapped additional oil immersed paper insulation.

References

1. Bejan FP (1994) Convective heat transfer, 2nd edn. Wiley, New York
2. Churchill SW, Chu HS (1975) Correlating equations for laminar and turbulent free convection from a horizontal cylinder. Int J Heat Mass Transfer 18:1049–1053
3. Morgan VT (1975) The overall convective heat transfer from smooth circular cylinder. Adv Heat Transfer 11:199–264
4. Gotter G (1954) Erwärmung und Kühlung elektrischer Maschinen. Springer, Berlin Heidelberg New York
5. Incropera FP, Dewitt DP (1996) Fundamentals of heat and mass transfer, 4th edn. Wiley, New York
6. IEC (1991) Loading guide for oil immersed transformers, 2nd edn. IEC Standard, Publication 60354
7. Seip GG (2000) Electrical installations handbook, 4th edn. Publicis MCD Verlag, Erlangen
8. Schaefer M, Feser K (1999) Thermal monitoring of large power transformers. In: Proceedings of the IEEE power tech 1999 conference, Budapest, paper nr. BPT99-072-30
9. Pradhan MK, Ramu TS (2003) Prediction of hottest spot temperature (HST) in power and station transformers. IEEE Trans Power Deliv 18:1275–1283
10. Radakovic Z, Feser K (2003) A new method for the calculation of the hot-spot temperature in power transformers with ONAN cooling. IEEE Trans Power Deliv 18:1284–1292